Journal of Low Temperature Physics
https://doi.org/10.1007/s10909-019-02152-3

Thermopower Quantum Oscillations in the Charge Density Wave State of the Organic Conductor α-(BEDT-TTF)$_2$KHg(SCN)$_4$

Danica Krstovska[1] · Eun Sang Choi[2] · Eden Steven[2,3]

Received: 22 October 2018 / Accepted: 21 January 2019

Abstract

We report on experimental studies of magnetic quantum oscillations of the interlayer thermopower in the charge density wave state of the multiband organic conductor α-(BEDT-TTF)$_2$KHg(SCN)$_4$. The magnetic field is along the direction perpendicular to the conducting layers. The interlayer thermopower or Seebeck effect has been measured in magnetic fields of up to 32 T and temperatures down to 0.5 K. The thermopower magnetic field dependence was measured at two temperatures 0.5 K and 4 K. Quantum oscillations observed in thermopower, at fields above 8 T and temperature 4 K, originate only from the α orbit, whereas at 0.5 K the energy spectrum consists of Landau levels of not only the α orbit but also the second harmonic as obtained from the fast Fourier transform analysis. In addition to the α and 2α frequencies, the oscillation spectrum reveals existence of a low-frequency peak at $F_\lambda = 180$ T which was previously observed in both magnetoresistance and magnetization. The behavior of thermopower magnetic quantum oscillations amplitude is analyzed using the Lifshitz–Kosevich formula, and the influence of different damping factors such as the temperature, spin splitting, Dingle and magnetic breakdown factors is studied. In addition, we analyze how the second harmonic of fundamental α frequency observed at low temperatures in the CDW$_0$ state at field perpendicular to the conducting layers affects the thermopower quantum oscillations amplitude. At low temperature, we find that on entering the low-field state, the scattering rate is observed to increase dramatically. We also observe an apparent increase in the effective mass of first harmonic from $m^*_\alpha = 1.7m_e$, in the low-field state to $m^*_\alpha = 3.3m_e$, in the high-field state. For the second harmonic, a constant effective mass of $m^*_{2\alpha} = 3.2m_e$ is estimated above and below the kink field.

Keywords Organic conductors · α-(BEDT-TTF)$_2$KHg(SCN)$_4$ · Interlayer thermopower · Magnetic quantum oscillations · Impurity scattering · Magnetic breakdown · Charge density wave

✉ Danica Krstovska
danica@pmf.ukim.mk; krstovska@magnet.fsu.edu

Extended author information available on the last page of the article

Published online: 07 February 2019

1 Introduction

The ground state of the quasi-two-dimensional organic conductor α-(BEDT-TTF)$_2$KHg(SCN)$_4$ has emerged as one of the more important fundamental problems in the area of synthetic metals. This is due to the highly unusual magnetic field-dependent behavior of the low-temperature ground state which appears below a transition temperature $T_p = 8$ K [1, 2]. The Fermi surface (FS) of this salt contains both a q2D cylinder and a pair of weakly warped open q1D sheets [3, 4]. The q1D and q2D bands are separated by a substantial gap near the Fermi level. At $T_p = 8$ K, the system undergoes a phase transition from metallic to an insulating charge density wave (CDW) state. The transition into the low-temperature phase (LTP) is associated with a $2k_F$ nesting instability of the q1D part of the Fermi surface. Indeed, experiments on the angle-dependent magnetoresistance oscillations [5–8] have revealed a significant change in the electronic system due to a periodic potential with the wave vector close to the doubled Fermi wave vector of the q1D band. It is important that the transition temperature T_p and, therefore, the relevant energy gap are much smaller than it is usually met in CDW materials. This leads to a very strong influence of a magnetic field on electronic properties, giving rise to numerous anomalies which stimulated high interest to this compound for over a decade. Although in the CDW phase no quasi-one-dimensional (q1D) FS sheet should survive, there appear clear angle-dependent magnetoresistance oscillations (AMRO) similar to the Lebed resonance, which is characteristic to q1D FS. Also, below T_p and at intermediate magnetic field ($B_k \sim$ 23 T), there are profound changes in the magnetoresistance which are indicative of a first-order phase transition in the electronic structure at the so-called kink transition field, B_k [9, 10]. The kink field B_k defines the high-field regime where the zero-field state CDW_0 is transformed into the CDW_x state with a field-dependent wave vector. This critical field clearly indicates that a magnetic field has a profound effect on the ground state of this compound.

In α-(BEDT-TTF)$_2$KHg(SCN)$_4$, de Haas–van Alphen (dHvA) and Shubnikov–de Haas (SdH) effects have been extensively studied in a number of articles at magnetic fields both well above and below the kink transition field B_k. For what concerns the magnetothermopower (thermopower and Nernst effect) behavior in α-(BEDT-TTF)$_2$KHg(SCN)$_4$, its magnetic field and angular dependences were experimentally obtained only for temperatures 4 K and 9 K [11, 12]. Although the background thermopower and Nernst effect were studied in detail, the magnetothermopower-related quantum oscillations have not been analyzed since at these temperatures they are suppressed due to the strong dependence on the thermal smearing of the FS. Advantages of thermopower include the zero-current nature of the measurement, and its sensitivity to band structure, especially in the case of anisotropic (low-dimensional FS) materials. The thermopower studies yield information about both the thermodynamic and transport properties of charge carriers and open new possibilities of studying the electronic structure of the organic conductors since the thermoelectric effects are significantly more sensitive to the electron energy spectrum than the galvanomagnetic effects.

Here we report on experimental studies of the magnetic quantum oscillations of interlayer thermopower in the charge density state of α-$(BEDT\text{-}TTF)_2KHg(SCN)_4$ when the temperature gradient is directed along the least-conducting axis in this material, the *b*-axis. In addition to the dominant α frequency corresponding to the large cylindrical Fermi surface predicted by the normal state band structure calculations [3, 4], a new, low frequency λ is found in the thermopower which was previously detected in both the SdH and dHvA spectra. The purpose of the present paper is to thoroughly investigate the thermopower magnetic quantum oscillations in the charge density state of the organic conductor α-$(EDT\text{-}TTF)_2KHg(SCN)_4$ by performing a detailed investigation of the field dependence of thermopower waveform and oscillation amplitude at magnetic fields both well above and below the kink transition field B_k.

2 Experiment

The single-crystal sample in this study was grown using conventional electrochemical crystallization techniques and was mounted on a rotating platform with a precision of a few degrees. Three pairs of Au wires were attached to the sample along the *b*-axis on the opposite sides of the *ac* planes of the sample with carbon paste for both the resistance and thermopower measurements. The resistance was measured by a conventional four-probe low-frequency lock-in technique. The usual experimental setup to measure the thermopower as a function of the magnetic field strength B and the angle between the field and normal to the layers θ is presented in Fig. 1. The sample was positioned between two quartz blocks, which were heated by sinusoidal heating currents with an oscillation frequency f_0 and phase difference $\pi/2$ to establish a small temperature gradient along the *b*-axis. The corresponding temperature gradient (∇T) and the thermal electromotive force (emf) with $2f_0$ oscillation frequency were measured for the thermopower or Seebeck signal. A miniature heater was placed on top of the sample to establish a small temperature gradient along the *b*-axis. The temperature gradient, which is found to be field independent, was set prior to each magnetic field sweep. For experimental inaccuracy to be minimal, which may result from the difference of temperature between the quartz block

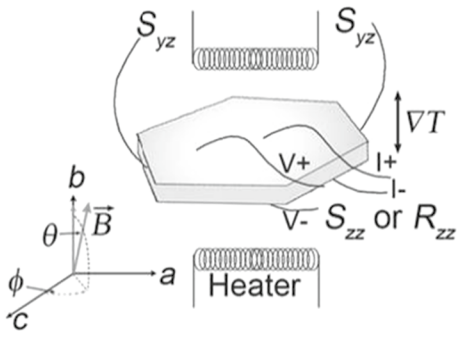

Fig. 1 Lead wire configuration and experimental geometry for the interlayer thermopower (Seebeck effect) and Nernst effect measurements in α -$(BEDT\text{-}TTF)_2KHg(SCN)_4$ as a function of the magnetic field strength and orientation

and the sample, the temperature gradient was produced by heating quartz blocks at a low frequency of 33 mHz. This experimental setup can be also used to measure the Nernst signal (for example, S_{yz} as shown in Fig. 1). For the purpose of our experiment, the thermopower is measured at two temperatures 0.5 K and 4 K in fields up to 32 T provided by the National High Magnetic Field Laboratory, Tallahassee, with a temperature gradient and magnetic field along the b-axis ($\nabla T \parallel b$, $\mathbf{B} \parallel b$) (Fig. 1). The same setup can be used to measure the thermopower and Nernst effect dependence on the polar angle θ, measured from the b-axis, and azimuthal angle ϕ, measured from the c-axis.

3 Results and Discussion

In general, thermopower contains two components: the background which is sensitive to the FS topology and an oscillatory component which is a manifestation of the Landau quantization of the closed orbit FS. In the following, we will consider the magnetic quantum oscillations of thermopower at temperatures 0.5 K and 4 K in the CDW state of organic conductor α-(BEDT-TTF)$_2$KHg(SCN)$_4$. Examples of the oscillatory magnetic thermopower of α-(BEDT-TTF)$_2$KHg(SCN)$_4$, measured in static magnetic fields of up to 32 T oriented along the least-conducting axis (b-axis) at temperatures 0.5 K and 4 K, are shown in Fig. 2. Theoretically obtained curves describing the thermopower oscillations that arise from the λ, α and 2α frequencies at 0.5 K (as seen from the fast Fourier transformation (FFT) of the data over a restricted range of B in Fig. 3a) and from λ and α at 4 K (Fig. 3b) are presented with the experimental curves in Fig. 4. The temperature and magnetic field dependences of the amplitude of observed frequencies in the thermopower quantum oscillations within both low- and high-magnetic field phases are presented in Figs. 5 and 6, respectively.

At low enough temperatures where the condition $\omega_c \tau \gg 1$ (ω_c being the cyclotron frequency and τ is the relaxation time) is satisfied, the quantization of the energy of electrons whose motion in the plane orthogonal to the magnetic field is finite should

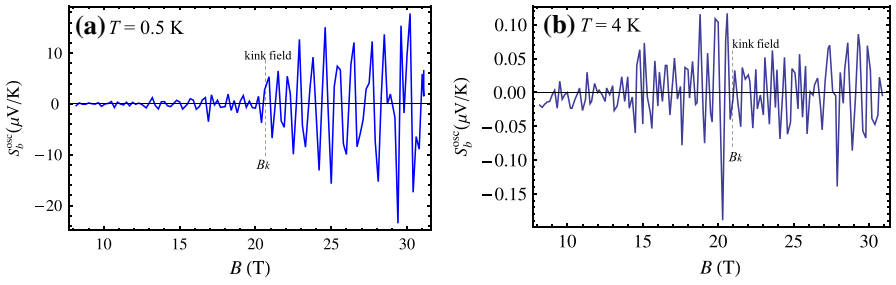

Fig. 2 Examples of experimentally measured magnetic quantum oscillations of interlayer thermopower $S_b^{osc}(B)$ are shown at **a** 0.5 K and **b** 4 K in both low- and high-field phases of α-(BEDT-TTF)$_2$KHg(SCN)$_4$. The kink field $B_k \sim 21$ T that defines the high-field regime where the zero-field state CDW_0 is transformed into the CDW_x state with a field-dependent wave vector is indicated by a dashed line (Color figure online)

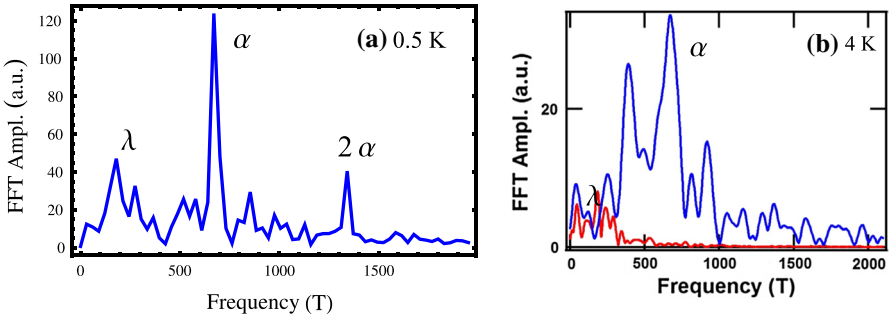

Fig. 3 Fast Fourier transformation of the data in Fig. 2 over a restricted range of B: **a** the field range is 12–27 T, **b** the red and blue curves correspond to a field range of 8–15 T and 15–30 T, respectively (Color figure online)

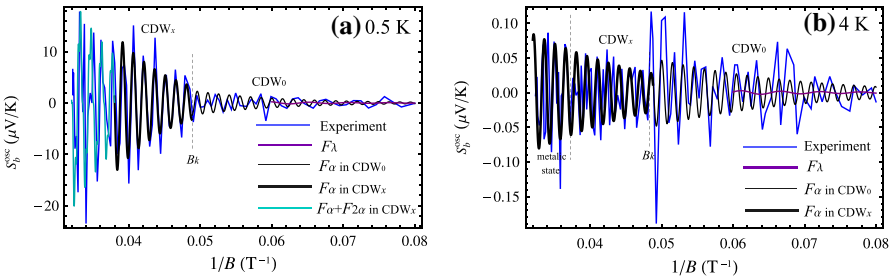

Fig. 4 Experimentally measured thermopower magnetic quantum oscillations in α-(BEDT-TTF)$_2$KHg(SCN)$_4$ (blue curves) and theoretically simulated curves based on LK model using the corresponding parameters as discussed in the text are presented at **a** 0.5 K and **b** 4 K as a function of the inverse magnetic field 1/B within both low- and high-magnetic field phases. The oscillations in **a** correlated with the low frequency λ (purple curve) and α frequency (black thin curve) below the kink field in the CDW$_0$ phase and α frequency (black thick curve) above the kink field in the CDW$_x$ phase are presented as obtained from the LK theory. The green curve that rather well fits the thermopower waveform at fields above $B = 26.5$ T corresponds to the combination of the fundamental α frequency and its second harmonic 2α in the LK model. The oscillations in **b** are correlated with the α frequency (black thin curve) and λ frequency (purple curve) below the kink field in the CDW$_0$ phase. Above the kink field in the CDW$_x$ phase α oscillations (black thick curve) are dominant (Color figure online)

be taken into account. Their states belong to the q2D closed orbits of the FS since the q1D part of the FS is an open orbit, and therefore does not undergo Landau quantization in the vicinity of the chemical potential μ. This part of the FS therefore behaves primarily as a carrier reservoir [13] to and from which the carriers can flow in an attempt to minimize the free energy of the system.

Regular quantum oscillations in thermopower continuously growing with field are observed above $B = 8$ T, the threshold field at which the α frequency oscillations emerge (Fig. 2). The kink field that defines the low-temperature CDW$_0$–CDW$_x$ phase transition is $B_k \sim 21$ T. The thermopower oscillations are more prominent at low temperatures as with increasing temperature they are suppressed due to the strong dependence on the thermal smearing of the Fermi surface. At 0.5 K, the

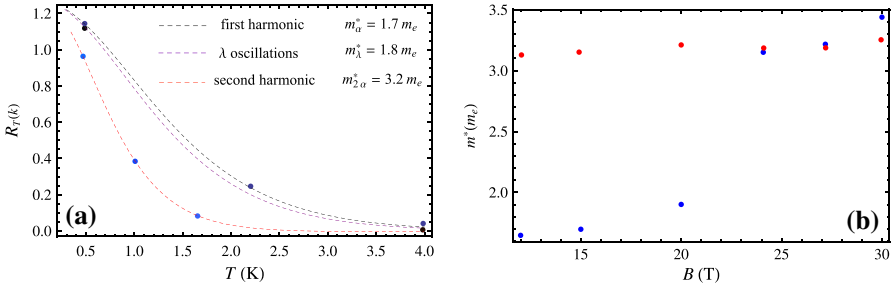

Fig. 5 **a** Temperature dependence of the first harmonic amplitude (dark blue symbols), second harmonic (light blue symbols) and λ oscillations (black symbols) at 15 T obtained by Fourier analysis of the thermopower data in this work. A fit to the R_T factor gives an effective mass of $m^*_\alpha = 1.7m_e$ (black dashed curve), $m^*_\lambda = 1.8m_e$ (purple dashed curve) and $m^*_{2\alpha} = 3.2m_e$ (red dashed curve), respectively. **b** Derived effective masses of the first harmonic (blue symbols) and second harmonic (red symbols) plotted as a function of magnetic field (Color figure online)

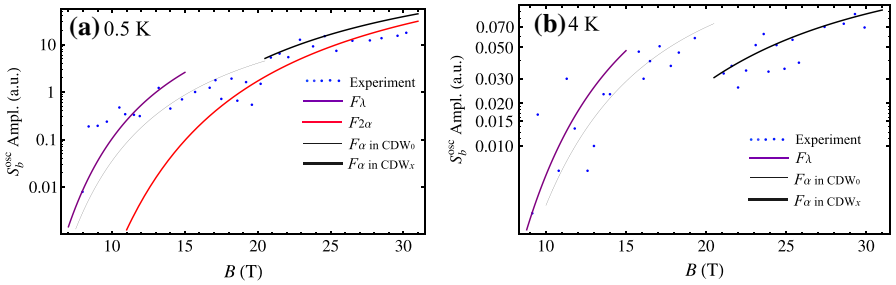

Fig. 6 Magnetic field dependence of the measured thermopower oscillation amplitude (blue symbols) in α-(BEDT-TTF)$_2$KHg(SCN)$_4$ at **a** 0.5 K and **b** 4 K. Solid curves are the field dependence of the oscillation amplitude based on the LK formula. The fitting in both cases is very good with using corresponding effective mass obtained from Fig. 5 and a Dingle temperature of **a** $T_D = 3.5$ K for α frequency below the kink field (black thin curve) and $T_D = 2.7$ K for α frequency above the kink field (black thick curve); $T_D = 3.7$ K for λ frequency below the kink field (purple curve) and $T_D = 1.5$ K for 2α frequency in both below and above the kink field (red curve). **b** $T_D = 0.2$ K for α frequency below the kink field (black thin curve) and $T_D = 0.5$ K for α frequency above the kink field (black thick curve) and $T_D = 0.5$ K for λ frequency below the kink field (purple curve) (Color figure online)

amplitude of the waveform is strongly damped within the low-magnetic field phase (CDW$_0$ phase), below B_k, usually associated with the kink field induced phase transition (Fig. 2a). At 4 K, a damping in the thermopower oscillation amplitude is seen not right below the kink field B_k but below fields of 15 T when the first harmonic is significantly attenuated (Fig. 2b).

In the present case, with the FFT analysis of the data in Fig. 2, we find that at $T =$ 0.5 K, the energy spectrum consists of Landau levels of the fundamental α orbit with frequency $F_\alpha = 671$ T, its second harmonic 2α with frequency $F_\alpha = 1342$ T and the slow oscillations with frequency $F_\lambda = 180$ T (Fig. 3a). At $T = 4$ K, there are only λ and α frequencies (Fig. 3b) that contribute to the thermopower waveform as expected since the second harmonic 2α, leading to splitting of the fundamental oscillations, was

found to emerge at temperatures below 2 K [5, 8, 14–17]. A number of articles have shown that the oscillations of the chemical potential μ (in this and other 2D materials) invalidates a simplistic analysis of the Shubnikov–de Haas (SdH) and de Haas–van Alphen (dHvA) oscillation data in terms of the Lifshitz–Kosevich (LK) formula [13, 18]. The reasons for this are twofold. First, the LK formula is suited only to systems in which the Fermi surface is significantly curved in all three k-spatial dimensions [13, 19]. Second, the oscillations of the chemical potential μ significantly perturb the waveform of the oscillations so as to cause the amplitude and sign of each of the $k>1$ harmonics to depart significantly from those predicted by the LK model [13]. In α-(BEDT-TTF)$_2$KHg(SCN)$_4$, quantum oscillations have proved to be especially sensitive to the kink transition field B_k [20]. It was also found that all signatures of a reconstructed Fermi surface are lost at high magnetic fields [21, 22], the effective mass m^* of the dominant α frequency appears to increase [21, 23–25], while the waveform is displaying split maxima at fields below B_k [15, 26]. In this work, we show that some of these trends are apparent in the thermopower oscillation data as well.

It is known that the waveform of the dHvA oscillations is significantly perturbed by μ in the canonical ensemble. In spite of this fact, the underlying sign and phase of the fundamental frequency (k=1) are the same as those in the grand canonical ensemble (or equivalently the LK model) for which μ is assumed to be constant [13, 19]. In our data, owing to the absence of a strong harmonic content in the signal, the thermopower waveform is determined mainly by the fundamental α frequency as the amplitudes of λ frequency and second harmonic 2α are much smaller than that of the fundamental (less than half of the amplitude of α frequency at 0.5 K while α frequency is the dominant one at 4 K). This is evident from the FFT spectra (Fig. 3) and allows to a degree of accuracy to neglect the oscillations of the chemical potential μ and use the grand canonical ensemble or the LK formula to calculate the thermopower waveform as well as the temperature and field dependence of the amplitude of thermopower oscillations.

The oscillatory part of the thermopower is determined mainly by the oscillatory dependence on the inverse magnetic field $1/B$ of the relaxation time $\tau(\varepsilon)$ that results from the summation over the electron states in the incoming term of the collision integral [27]. In the Born approximation, for $\hbar\omega_c \ll t_c$, the relaxation time is given by

$$\frac{1}{\tau(\varepsilon)} = \frac{1+\Delta_{\mathrm{osc}}}{\tau_0}, \tag{1}$$

where the oscillatory part is

$$\Delta_{\mathrm{osc}} = \left(\frac{\hbar eB}{t_c m^*}\right)^{1/2} \sum_{k=1}^{\infty} \frac{(-1)^k}{k^{1/2}} R_T(k\Lambda) R_S(k) R_{\mathrm{D}}(k) R_{\mathrm{MB}}(k) \cos\left(\frac{kS_{\mathrm{ext}}}{e\hbar B} \pm \frac{\pi}{4}\right). \tag{2}$$

Here, $\hbar$ is the Planck constant divided by 2π, τ_0 is the nonoscillatory part of the relaxation time, t_c is the interlayer transfer integral, k_B is the Boltzmann constant and S_{ext} is the extremal cross section of the Fermi surface by the plane $p_B = \mathrm{const}$ and m^* is the cyclotron mass. The corresponding spread of the Fermi surface areas due to temperature will lead to a smearing of the phase, which in turn will reduce the oscillation amplitude. This factor is written as

$$R_T(k\Lambda) = \frac{k\Lambda\left(\frac{m^*}{m_e}\right)\frac{T}{B}}{\sinh\left(k\Lambda\left(\frac{m^*}{m_e}\right)\frac{T}{B}\right)}, \tag{3}$$

where $\Lambda = 2\pi^2 k_B m_e/\hbar e \sim 14.96$ T/K and m_e is the free electron mass. The reduction in the amplitude from the Zeeman spin splitting is described by the damping factor $R_S(k) = \cos(k\frac{\pi}{2}g(m^*/m_e))$ where g is the conduction electron g-factor. A reduced amplitude can also result from the electron scattering on impurities. Determination of the so-called Dingle factor $R_D(k) = \exp(-k\Lambda(m^*/m_e)T_D/B)$ provides information on the purity and crystal quality of a measured sample. In high enough magnetic fields, it is possible for two conducting bands near a Fermi level to come close enough to each other for the electrons to tunnel from one band into the other. This phenomenon is called magnetic breakdown (MB). The change in the bands can be seen as switching between different orbits on the Fermi surface leading to, e.g., a change in the cyclotron frequency and the effective mass. The magnetic breakdown damping factor is expressed as $R_{MB}(k) = \exp(-kB_{MB}/B)$ where B_{MB} is the magnetic breakdown field.

The thermopower is determined by performing a derivative of the density of states (DoS) over μ, and therefore, the amplitude of the oscillations can be written in the following form

$$\begin{aligned} S_b^{osc} = &\frac{\pi^2 k_B T}{3e}\mu\left(\frac{m^*}{t_c\hbar e}\right)^{1/2}\frac{1}{B^{1/2}}\sum_{k=1}^{\infty}(-1)^k k^{3/2} R_T(k\Lambda)R_S(k)R_D(k)R_{MB}(k) \\ &\times \sin\left(2\pi k\left(\frac{F}{B}-\frac{1}{2}\right)\right), \end{aligned} \tag{4}$$

where $F = \mu\, m^*/\hbar e$ is the oscillation frequency.

Using eq. (4), we find that in our experiment the thermopower waveform is well described in the frame of the grand canonical ensemble. A reasonable fit to the experimental thermopower waveform (with the inverse magnetic field 1 / B) presented in Fig. 4 is achieved using the experimentally obtained parameters such as the effective mass, Dingle temperature (or scattering rate) and a magnetic breakdown field of $B_{MB} \sim 5$ T. The details are discussed below.

At both temperatures, the thermopower oscillations are dominated by the fundamental α oscillations which result from the magnetic breakdown. The λ oscillations come from a classical small orbit formed after the Fermi surface reconstruction. At low fields around 8 T, the amplitudes of the λ and α oscillations are comparable. With increasing field, the contribution of the λ frequency decreases due to the enhancement of the α oscillations as a result of increase in the breakdown probability. Above 17 T, the contribution of the λ frequency to the thermopower magnetic quantum oscillations diminishes as the MB is strong at fields close to the kink field B_k. This is in a good agreement with previous reports obtained from the SdH and dHvA oscillations [28]. The grand canonical ensemble (i.e., the LK model which assumes a fixed chemical potential) calculation is able to reproduce the

experimentally observed thermopower field dependence in Fig. 4 rather well in both low- and high-field phases.

In order to reproduce the thermopower waveform from the experiment in the frame of LK model, one has to estimate effective mass and Dingle temperature (or scattering rate) of the oscillations observed in the FFT spectrum. Fits of the thermopower oscillation amplitude to the temperature damping factor R_T (at constant magnetic field B) provide the best estimate of the effective mass. In our analysis, all amplitudes of the quantum oscillations were obtained by Fourier analysis over short intervals of reciprocal field space with the short data sets. A typical fit is shown in Fig. 5a at $B = 15$ T. The derived effective masses of the oscillations analyzed as a function of magnetic field allow to estimate their values below and above the kink field (Fig. 5b). We find that the effective mass of α frequency is enhanced as the magnetic field drives the sample through the kink transition. The effective mass of first harmonic is obtained by a direct fit to the LK formula and is field dependent, as is the Dingle temperature (see the text). In contrast, the effective mass of the second harmonic is found to be field independent with the transition between the phases. We find that at $T = 0.5$ K, within the CDW_0 phase $m^*_\alpha = 1.7m_e$, whereas in the CDW_x phase $m^*_\alpha = 3.3m_e$ (Fig. 5b).

For the λ orbit, observed only in the CDW_0 phase, we obtain an effective mass of $m^*_\lambda = 1.8m_e$. We should note that in our experiment the λ oscillations effective mass m^*_λ is close in value to the first harmonic effective mass m^*_α below the kink field, but the estimate made for m^*_λ has a greater error due to relatively low amplitude of λ oscillations compared to that of the first harmonic. For the second harmonic, a constant effective mass of $m^*_{2\alpha} = 3.2m_e$ is estimated above and below the kink field (Fig. 5b). We attribute this to the small second harmonic amplitude compared to that of the fundamental within the low-magnetic field phase. The effective mass of second harmonic is around double that of the first harmonic in the CDW_0 phase which is consistent with the LK model. Usually, different values of the effective mass are obtained in the CDW_0 phase depending on whether one analyzes SdH or dHvA data [23]. Some of the values obtained in this work are consistent with those derived from the SdH data and others with those from dHvA measurements [8, 22–25]. This is, however, expected since thermopower contains information about both the thermodynamic and transport properties of charge carriers.

There have been attempts to explain whether the apparent change in the effective mass of the α frequency on crossing B_k is related to a change in the strength of the *e–ph* interactions (since CDW ground states are commonly thought to involve *e–ph* interactions rather than *e–e* interactions), or whether it is an artifact of the temperature dependence of the condensate. In Reference [29], the authors eliminate both impurity scattering and magnetic breakdown as dominant mechanisms for the reduction in the amplitude within the CDW_0 phase. It is shown that damping is not indexed to the harmonics which appears to be the case when the effective volume of the sample contributing to the dHvA signal is field dependent within the CDW_0 phase. In this work, with thermopower measurements, we find that both mechanisms play an important role in damping of the waveform below B_k, but their impact on damping of each harmonic is different and temperature dependent. In contrast to the fairly gentle decrease in amplitude observed for the first harmonic in the CDW_0

phase, the second harmonic shows a more abrupt change as previously find in Reference [23]. This implies that the amplitude attenuation is indexed to the harmonics. Furthermore, thermopower quantum oscillations measurements reveal that at low temperatures split waveform due to spin splitting occurs only at fields $B \geq 26.5$ T in the high-field phase (CDW_x phase). At these fields, the waveform is reproduced rather well as a combination of the oscillations of fundamental α frequency and its second harmonic 2α in the LK model. This correlates with previous findings that spin splitting does not occur within the low-magnetic field phase (CDW_0 phase) until the angle between the magnetic field and the normal to the conducting planes is 42° implying that not electron–electron but electron–phonon interactions play a significant role in the formation of the charge density wave ground state. We note that the g-factor for the conduction electrons is a fixed fitting parameter in our model, $g = 1.8$. With this and the apparent change in the effective mass of the α frequency, we find that a single value for the product of the effective mass with the electron g-factor cannot explain the experimental data deep within both the high-magnetic field and low-magnetic field phases. This further confirms that the amplitude damping is indeed indexed to the harmonics.

One of the features of the thermopower technique (in addition to the dHvA one) is that it allows the determination of scattering rates, τ^{-1}, for the charge carriers residing on different parts of the Fermi surface. This is done by measuring the amplitude of different orbits as a function of magnetic field (Fig. 6) to determine the Dingle temperature $T_D = \hbar/2\pi k_B \tau$. Clearly, at 0.5 K, the second harmonic 2α is present in both low- and high-field phases but with an amplitude that is roughly two orders of magnitude smaller than that of the fundamental. We find that the transition from the CDW_x to CDW_0 phase is characterized with an increase in the Dingle temperature T_D or equivalent to an increase in the scattering rate τ^{-1}. A number of groups have already reported an apparent increase in the scattering rate within the low-magnetic field phase (CDW_0 phase) with respect to that within the high magnetic field (CDW_x phase) [23, 24]. In this work, at $T = 0.5$ K (Fig. 6a), a Dingle temperature T_D of 2.7 K in the CDW_x yields a scattering rate of $\tau^{-1} = 2.2 \times 10^{12}\ s^{-1}$ for the first harmonic, while a T_D of 3.5 K in the CDW_0 phase yields a scattering rate of $\tau^{-1} = 2.9 \times 10^{12}\ s^{-1}$, comparable to those obtained in Reference [23].

Similarly, for the λ oscillations, a Dingle temperature of $T_D = 3.7$ K corresponds to $\tau^{-1} = 3 \times 10^{12}\ s^{-1}$, whereas for the 2α oscillations a $T_D = 1.5$ K yields $\tau^{-1} = 1.2 \times 10^{12}\ s^{-1}$. The large quasiparticle scattering rate below the kink field is observed in both the first and second harmonics, indicating that additional quasiparticle scattering processes come into existence below the kink field compared to the high-field state; these additional scattering processes are possibly associated with the formation of the CDW. Our results show that, in the low-field phase, the first harmonic is much more affected by the impurity scattering than the second harmonic since the scattering rate for the former is around double that of the latter.

The magnetic breakdown probability has also an influence on the amplitude of the individual oscillation. Some authors have already attributed the loss of amplitude of the α frequency within the CDW_0 phase in α-$(BEDT\text{-}TTF)_2KHg(SCN)_4$ to the magnetic breakdown effects [25, 30]. Here we analyze the influence of magnetic breakdown effect on thermopower oscillations. From the kink field $B_k \sim 21$

T of the low-temperature CDW_0–CDW_x phase transition, we find that the energy gap separating the open and closed parts of the Fermi surface $\Delta_{CDW} \sim \mu_B B_k$ is of order $\Delta_{CDW} = 3.8$ eV. This yields a breakdown field of $B_{MB} \sim 5$ T. The magnetic breakdown definitely contributes to the loss of oscillation amplitude of both fundamental and second harmonics within the CDW_0 phase, but the large scattering rates obtained at low temperature and given small breakdown field indicate that at 0.5 K the impurity scattering is more prominent in harmonic amplitude reduction even more for the first harmonic.

At 4 K (Figs. 2b, 4b), the thermopower waveform is determined by the α oscillations without a rapid damping in the amplitude below the kink field. This is associated with the slight change in the first harmonic effective mass with the transition from CDW_x to CDW_0 phase. Indeed, the effective mass of α oscillations changes from $m_\alpha^* = 1.5m_e$ within the CDW_x phase to $m_\alpha^* = 1.2m_e$ in the CDW_0 phase (Fig. 5). A Dingle temperature of $T_D = 0.2$ K below the kink field yields a scattering rate of $\tau^{-1} = 1.65 \times 10^{11}\ s^{-1}$, whereas a $T_D = 0.5$ K above the kink field corresponds to $\tau^{-1} = 4 \times 10^{11}\ s^{-1}$ (Fig. 6b). For the λ frequency, the values are close to those of α frequency in the CDW_0 phase: $m_\lambda^* = 1.2m_e$, $T_D = 0.5$ K. We should note that at 4 K the material is in the CDW_x phase only within a narrow field region of B, 21.1 $T < B <$ 26.5 T, while above 26.5 T it is in the normal metallic state. Also, the first harmonic is significantly attenuated in fields below 15 T as obtained from the FFT analysis of the thermopower data over the field range 8–15 T (red curve in Fig. 3b). This might be due to the rapid decrease in the total thermopower at this temperature below the maximum field $B_{max} = 15$ T [11]. At 4 K, the scattering rate for the first harmonic is much lower compared to that at 0.5 K, especially in the low-field phase. This implies that at higher temperatures the influence of impurity scattering on amplitude reduction would be much smaller compared to that at lower temperatures, but on the other hand, the magnetic breakdown effect might become significant. In fields above the kink field B_k, the CDW gap is considerably reduced and, given, additionally, a strong MB, the thermopower behavior should be similar to that in the normal state. However, our data reveal features which are distinct from the normal metallic properties but consistent with the CDW scenario. Comparing the thermopower amplitude in both CDW_0 and CDW_x phases, one can see that the thermopower in the high-field state resembles that of the CDW_0 phase. Indeed, for fields 21.1 T< $B <$ 26.5 T the thermopower amplitude is of the same order in magnitude as in the narrow field region 15.8 T< $B <$ 18.8 T in the CDW_0 phase right below the transition. This, however, suggest that there is a bigger similarity between the low- and high-field phases than expected implying that the open FS sheets might still survive in the CDW_x phase. On the other hand, we obtain one value for the first harmonic effective mass and scattering rate at fields above B_k, for the CDW_x and normal metallic phases (and additionally, smaller first harmonic amplitude above B_k). This indicates that the thermopower in the high-field phase should also reflect some of the properties of the normal metallic state. Such a behavior was previously observed in the angular dependence of total thermopower of α-$(BEDT\text{-}TTF)_2KHg(SCN)_4$ [12]. Thus, here obtained results from the thermopower quantum oscillations measurements at higher temperatures corroborate and advance previous findings

on possible FS reconstruction in this organic conductor at fields right above the kink field B_k.

4 Conclusions

We report the results of a detailed study of the thermopower waveform and oscillation amplitude field dependence in the charge density wave state of the organic conductor α-(BEDT-TTF)$_2$KHg(SCN)$_4$ at temperatures 0.5 K and 4 K. The thermopower waveform and oscillation amplitude are analyzed below and above the kink transition field $B_k \sim 21$ T, i.e., in both low-magnetic field phase (CDW_0) and high-magnetic field phase (CDW_x), by applying the grand canonical ensemble (or LK model) to investigate the damping of the amplitude due to temperature, impurity scattering, spin splitting and magnetic breakdown effects. We find that the thermopower waveform and amplitude are fairly well reproduced within the model at both temperatures mostly because the oscillation spectrum is dominated by the fundamental α frequency. The low frequency λ is observed in thermopower oscillations only in the CDW_0 phase, whereas the second harmonic 2α is present in both CDW_0 and CDW_x phases only at 0.5 K. There is a rapid attenuation of the thermopower waveform at low temperature below B_k in the CDW_0 phase, while at higher temperature a damping of the amplitude is observed in the CDW_x phase. We find that there is an apparent enhancement of the effective mass of the first harmonic with the transition from CDW_0 to CDW_x phase at both temperatures. On the other hand, we observe an increase in the scattering rate in the CDW_0 phase at 0.5 K opposite of the case of 4 K where the scattering rate is much lower and increases with the CDW_0–CDW_x transition. In addition, the magnetic breakdown effect also reduces the amplitude, but at low temperature its impact is smaller than that of the impurity scattering mechanism. On the other hand, at high temperature magnetic breakdown effect might be significant in the amplitude damping within the CDW_0 phase. The spin splitting of the thermopower oscillations is observed only at low temperatures and high fields and is well reproduced as a combination of the first and second harmonics in the LK model. At higher temperature, there is an apparent decrease in the oscillation amplitude above B_k, but the results are fitted with one value for the α frequency effective mass in the CDW_x and normal metallic phase. This implies that there are similarities between both phases. However, in a narrow field range just above B_k the thermopower amplitude is similar in value of that in the CDW_0 just below the B_k. This suggests that the high-field phase might reflect the properties of both CDW_0 and metallic states.

Acknowledgements The work was performed at the National High Magnetic Field Laboratory, supported by NSF DMR-0654118, by the State of Florida, and by the DOE.

References

1. M.V. Kartsovnik, *The Physics of Organic Superconductors and Conductors* (Springer, Berlin, 2008)

2. P. Foury-Leylekian, J.P. Pouget, Y.J. Lee, R.M. Nieminen, P. Ordejón, E. Canadell, Phys. Rev. B **82**, 134116 (2010)
3. H. Mori, S. Tanaka, M. Oshima, G. Saito, T. Mori, Y. Maruyama, H. Inokuchi, Bull. Chem. Soc. Jpn. **63**, 2183 (1990)
4. R. Rousseau, M.L. Doublet, E. Canadell, R.P. Shibaeva, S.S. Khasanov, L.P. Rozenberg, N.D. Kushch, E.B. Yagubskii, J. Phys. I Fr. **6**, 1527 (1996)
5. M.V. Kartsovnik, A.E. Kovalev, N.D. Kushch, Phys. I Fr. **3**, 1187 (1993)
6. A.E. Kovalev, M.V. Kartsovnik, R.P. Shibaeva, L.P. Rozenberg, I.F. Schegolev, N.D. Kushch, Solid State Commun. **89**, 575 (1994)
7. T. Sasaki, N. Toyota, Phys. Rev. B **49**, 10120 (1994)
8. J. Caulfield, S.J. Blundell, M.S.L. du Croo, P.T.J. de Jongh, J. Hendriks, M. Singleton, F.L. Doporto, A. Pratt, J.A.A.J. House, W. Perenboom, M. Hayes, M. Kurmoo, P. Day, Phys. Rev. B **51**, 8325 (1995)
9. J.S. Qualls, L. Balicas, J.S. Brooks, N. Harrison, L.K. Montgomery, M. Tokumoto, Phys. Rev. B **62**, 10008 (2000)
10. C. Proust, A. Audouard, A. Kovalev, D. Vignolles, M. Kartsovnik, L. Brossard, N. Kushch, Phys. Rev. B **62**, 2388 (2000)
11. D. Krstovska, E. Steven, E.S. Choi, J.S. Brooks, Low Temp. Phys. **37**, 950 (2011)
12. D. Krstovska, E.S. Choi, E. Steven, J.S. Brooks, J. Phys. Condens. Matter **24**, 265502 (2012)
13. N. Harrison, R. Bogaerts, P.H.P. Reinders, J. Singleton, S.J. Blundell, F. Herlach, Phys. Rev. B **54**, 9977 (1996)
14. J.S. Brooks, S.J. Klepper, C.C. Agosta, M. Tokumoto, N. Kinoshita, Y. Tanaka, S. Uji, H. Aoki, G.J. Athas, X. Chen, H. Anzai, Synth. Met. **56**, 1791 (1993)
15. M. Tokumoto, A.G. Swanson, J.S. Brooks, C.C. Agosta, S.T. Hannahs, N. Kinoshita, H. Anzai, J.R. Anderson, J. Phys. Soc. Jpn. **59**, 2324 (1990)
16. M.V. Kartsovnik, A.E. Kovaleva, V.N. Laukhin, S.I. Pesotskii, N.D. Kushch, JETP Lett. **55**, 339 (1992)
17. A. House, C.J. Hawoth, J.M. Caulfield, S. Blundell, M.M. Honold, J. Singleton, W. Hayes, S.M. Hayden, P. Meeson, M. Springford, M. Kurmoo, P. Day, J. Phys. Condens. Matter **8**, 10361 (1996)
18. N. Harrison, C.H. Mielke, D.G. Rickel, J. Wosniza, J.S. Qualls, J.S. Brooks, E. Balthes, D. Shweitzer, I. Heinen, W. Strunz, Phys. Rev. B **98**, 10248 (1998)
19. D. Shoenberg, *Magnetic Oscillations in Metals* (Cambridge University Press, Cambridge, 1984)
20. T. Osada, R. Yagi, A. Kawasumi, S. Kagoshima, N. Miura, M. Oshima, G. Saito, Phys. Rev. B **41**, 5428 (1990)
21. T. Sasaki, A.G. Lebed, T. Fukase, N. Toyota, Phys. Rev. B **54**, 12969 (1996)
22. N. Harrison, L. Balicas, J.S. Brooks, M. Tokumoto, Phys. Rev. B **62**, 14212 (2000)
23. N. Harrison, A. House, I. Deckers, J. Caulfield, J. Singleton, F. Herlach, W. Hayes, M. Kurmoo, P. Day, Phys. Rev. B **52**, 5584 (1995)
24. P. Christ, W. Biberacher, H. Müuller, K. Andres, E. Steep, A.G.M. Jansen, Physica B **204**, 153 (1995)
25. S. Uji, J.S. Brooks, M. Chaparala, L. Seger, T. Szabo, M. Tokumoto, N. Kinoshita, T. Kinoshita, Y. Tanaka, H. Anzai, Solid State Commun. **100**, 825 (1996)
26. T. Sasaki, N. Toyota, Phys. Rev. B **48**, 11457 (1993)
27. A.A. Abrikosov, *Fundamentals of the Theory of Metals*, 2nd edn. (North-Holand, Amsterdam, 1988)
28. M.V. Kartsovnik, V.N. Zverev, D. Andres, W. Biberacher, T. Helm, P.D. Grigoriev, R. Ramazashvili, N.D. Kushch, H. Müller, Low Temp. Phys. **40**, 377 (2014)
29. N. Harrison, N. Biskup, J.S. Brooks, L. Balicas, M. Tokumoto, Phys. Rev. B **63**, 195102 (2001)
30. T. Sasaki, W. Biberacher, T. Fukase, Physica B **246–247**, 303 (1998)

Affiliations

Danica Krstovska[1] · Eun Sang Choi[2] · Eden Steven[2,3]

[1] Faculty of Natural Sciences and Mathematics, Ss. Cyril and Methodius University, 1000 Skopje, Macedonia

[2] National High Magnetic Field Laboratory, Florida State University, Tallahassee, FL 32310, USA

[3] Emmerich Education Center, Jakarta, Indonesia